

## Toll-like receptor 4: a target for chemoprevention of hepatocellular carcinoma in obesity and steatohepatitis

Jennifer Nguyen<sup>1</sup>, Jingjing Jiao<sup>1</sup>, Kristin Smoot<sup>1</sup>, Gordon P. Watt<sup>1,2</sup>, Chen Zhao<sup>1</sup>, Xingzhi Song<sup>3</sup>, Heather L. Stevenson<sup>4</sup>, Joseph B. McCormick<sup>2</sup>, Susan P. Fisher-Hoch<sup>2</sup>, Jianhua Zhang<sup>3</sup>, P. Andrew Futreal<sup>3</sup> and Laura Beretta<sup>1</sup>

<sup>1</sup>Department of Molecular and Cellular Oncology, The University of Texas MD Anderson Cancer Center, Houston, TX, USA

<sup>2</sup>University of Texas Health Science Center at Houston, School of Public Health in Brownsville, Brownsville, TX, USA

<sup>3</sup>Department of Genomic Medicine, Division of Cancer Medicine, The University of Texas MD Anderson Cancer Center, Houston, TX, USA

<sup>4</sup>Department of Pathology, The University of Texas Medical Branch, Galveston, TX, USA

**Correspondence to:** Laura Beretta, email: lberetta@mdanderson.org

**Keywords:** toll-like receptor 4; chemoprevention; NAFLD; hepatocellular carcinoma; mouse model

**Received:** April 07, 2018

**Accepted:** June 13, 2018

**Published:** June 29, 2018

**Copyright:** Nguyen et al. This is an open-access article distributed under the terms of the Creative Commons Attribution License 3.0 (CC BY 3.0), which permits unrestricted use, distribution, and reproduction in any medium, provided the original author and source are credited.

### ABSTRACT

**The incidence of hepatocellular carcinoma (HCC) associated with non-alcoholic fatty liver disease (NAFLD) is rapidly increasing. We aimed to elucidate the genetic basis of NAFLD-associated HCC and identify candidate targets for chemoprevention. Twenty HCC tumors, distant liver and matched tails from mice with hepatocyte-deletion of Pten (Hep<sup>Pten</sup><sup>-/-</sup>) were subjected to whole-exome sequencing. A total of 162 genes with somatic non-synonymous single nucleotide variants or exonic small insertions and deletions in tumors were identified. Ingenuity Pathway Analysis of these 162 genes, further identified Toll-like receptor (TLR) 4, a key mediator of proinflammatory responses, and resatorvid, a TLR4 inhibitor, as the main causal networks of this dataset. Resatorvid treatment strongly prevented HCC development in these mice ( $p < 0.001$ ). Remarkably, HCC patients with high tumoral TLR4 mRNA expression were more likely to be diagnosed with NAFLD and obese. TLR4 mRNA expression positively correlated with IL-6 and IL-10 mRNA expression in HCC tumors and the correlation was stronger in obese HCC patients. We have identified tumor mutation signatures and associated causal networks in NAFLD-associated HCC in Hep<sup>Pten</sup><sup>-/-</sup> mice and further demonstrated the important role of TLR4 in promoting HCC development. This study also identified IL-6 and IL-10 as markers of TLR4 activation in HCC and subjects with NAFLD and obesity as the target population who would benefit from TLR4 inhibition treatment for HCC chemoprevention.**

### INTRODUCTION

Hepatocellular carcinoma (HCC) is the second leading cause of cancer-related mortality worldwide [1]. In the United States, HCC incidence and mortality rates are rapidly increasing, in part due to the epidemics of obesity and diabetes, leading to non-alcoholic fatty liver disease (NAFLD) [2, 3]. NAFLD is a spectrum of diseases that begins with simple steatosis and eventually progresses to steatohepatitis (NASH), leading to cirrhosis and HCC [4].

Most patients with HCC are diagnosed at an advanced stage when limited treatment options are available, often due to the presence of cirrhosis and poor liver function. Hence, the development of novel therapeutic options for the treatment of NASH and prevention of HCC is urgently needed [5, 6].

In this study, we aimed to elucidate the genetic basis of NAFLD-associated HCC and identify candidate targets for chemoprevention. To that end, we performed whole-exome sequencing on tumors and used Ingenuity Pathway

Analysis (IPA) to identify candidate genetic drivers of HCC in a mouse model of NASH-related HCC. We further validated the main candidate target in HCC prevention studies *in vivo* and characterized the target's expression in human HCCs. Mouse models are extensively used and readily accessible sources of invaluable information when developing therapeutic strategies for human diseases. Mouse models for target discovery should reproduce the natural pathogenesis of the human disease of interest. We used mice with hepatocyte-specific Pten deletion (Hep<sup>Pten</sup><sup>-</sup>). Hep<sup>Pten</sup><sup>-</sup> mice develop steatosis, liver fibrosis, NASH and HCC [7, 8]. This model most closely resembles both the histopathology of and the molecular changes associated with human NASH and HCC [9]. In addition, human NASH and HCC are characterized by PTEN mutations, inhibition of PTEN expression, or loss of PTEN function [10, 11].

## RESULTS

### Whole-exome sequencing of HCCs and Ingenuity Pathway Analysis identified TLR4 as a candidate target for HCC prevention in Hep<sup>Pten</sup><sup>-</sup> mice

To elucidate the genetic basis of NASH-associated HCC and identify candidate targets for chemoprevention, 20 HCC tumors, distant liver and matched tails collected from ten male mice with hepatocyte-deletion of Pten (Hep<sup>Pten</sup><sup>-</sup>) were subjected to whole-exome sequencing (WES). Somatic single nucleotide variants (SNVs) and small insertions and deletions (indels) were identified by comparing tumor or distant nontumor liver samples to tails. A total of 90 somatic non-synonymous single nucleotide variants (SNVs) and 80 exonic small insertions and deletions (indels) covering 162 genes were identified in tumors. The co-mutation data of each HCC tumor is shown in Supplementary Table 1. Among these 162 genes, 8 were also mutated in the adjacent non tumoral liver. The number of mutations detected in each tumor ranged from 2 to 25 with an average of 10 mutations per tumor. The highest frequency (3 out of 20 tumors) was observed for a frameshift insertion mutation in the FK506 binding protein 7, *Fkbp7* (A129fs). Genes mutated in 2 out of the 20 tumors were *Atp5g3*, *Cdh7*, *Dennd2a*, *Esco2*, *Fndc3a*, *Gm1995*, *Gopc*, *Grb10*, *Mdc1*, *Nop58*, *Polr3c*, *Senp6*, *Serpinb3a*, *Serpinb3b*, *Serpinb3d*, *Spice1*, *Stxbp3a*, *Xylt2*, and *Zzef1*. All other genes were found mutated in a single tumor and included known drivers of hepatocarcinogenesis such as *Birc6*, *Hras*, and *Kmt2a*. Among these 162 genes, 119 were found mutated in HCC in TCGA HCC database, representing 64% of all HCCs.

To identify potential therapeutic targets, the list of the 162 genes was uploaded onto Ingenuity Pathway Analysis (IPA) software for upstream and causal network analysis. Core Analysis by IPA identified 5 top upstream regulators that directly target genes from the

dataset: NK2 homeobox 5 (NKX2-5) ( $p = 9.26 \times 10^{-5}$ ), fucosyltransferase 7 (FUT7) ( $p = 3.85 \times 10^{-4}$ ), Yin-Yang 1 associated protein 1 (YY1AP1) ( $p = 5.76 \times 10^{-4}$ ), interleukin 10 receptor alpha (IL10RA) ( $p = 7.43 \times 10^{-4}$ ) and stromal-derived factor 1 (CXCL12) ( $p = 1.32 \times 10^{-3}$ ) (Figure 1A). To further evaluate the relevance of the identified top upstream regulators, we sought to determine the mutation distribution of target genes in each network in the Hep<sup>Pten</sup><sup>-</sup> model as well as in human HCCs using the cBioPortal-TCGA HCC database (Figure 1B–1C). For each upstream regulator, 2 to 8 target genes were found mutated in Hep<sup>Pten</sup><sup>-</sup> tumors. These include *Hand1*, *Ifi16*, *Mylk*, and *Ryr2* regulated by upstream *Nkx2-5*; *Add3*, *Aldob*, *Ca2*, *Ctse*, *Cyp2s1*, *Ifi16*, and *Ikbke* regulated by upstream *Il10ra*; *Ca2*, *Gopc*, *Itgb1*, *Ryr2*, *Selplg*, and *Yyl* regulated by upstream *Cxcl12* (*SDF1*); and *Nf2* and *Yyl* regulated by upstream *Yylap1* (*Hcca2*) (Figure 1B). These 4 altered networks were detected in 20–40% of Hep<sup>Pten</sup><sup>-</sup> mice and in 1.3–13% of human HCCs (Figure 1B–1C).

Core Analysis by IPA also identified significant causal networks. The top four causal networks were all found to be closely associated with toll-like receptor (TLR) 4 (Figure 1A). Resatorvid ( $p = 2.51 \times 10^{-6}$ ) is a small molecule that specifically inhibits TLR4 by binding to Cys<sup>747</sup> in the intracellular TIR domain of TLR4 [12]. Single immunoglobulin interleukin-1 receptor related molecule (SIGIRR) ( $p = 2.98 \times 10^{-5}$ ) inhibits TLR4 signaling through interaction with TLR4, MD2, MyD88, and TIRAP [13]. TLR2/TLR4 ( $3.18 \times 10^{-5}$ ) are both implicated in recognizing various bacterial cell wall components and both signal an inflammatory response through MyD88 [14]. CD14 and LY96 ( $p = 3.50 \times 10^{-5}$ ) are adaptor proteins that assist in maneuvering ligands to TLR4 [15]. Based on these results, TLR4 was identified as the main driver of HCC development in Hep<sup>Pten</sup><sup>-</sup> mice and resatorvid as the main candidate therapeutic drug for the prevention of NASH-associated HCC.

### Resatorvid prevented HCC development in Hep<sup>Pten</sup><sup>-</sup> mice

We then investigated whether resatorvid treatment could prevent HCC development in Hep<sup>Pten</sup><sup>-</sup> mice. Because HCC develop in male Hep<sup>Pten</sup><sup>-</sup> mice between 8 and 9 months of age, we selected for the study nineteen 8-month old male mice with no tumors as confirmed by MR imaging (MRI) and separated them into a placebo group ( $n = 10$ ) and a resatorvid-treated group ( $n = 9$ ). Hep<sup>Pten</sup><sup>-</sup> were treated with resatorvid daily for 28 days with intraperitoneal injections of 10 mg/kg and mice were imaged by MRI at day 0, day 14 and day 28. Representative MRI images of tumors detected at day 28 are shown in Figure 2A. At day 14, no tumor could be detected in the resatorvid-treated mice while 5 of the 10 placebo mice developed 1 or 2 tumors ( $p = 0.022$ ). At day 28, up to 3 tumors were detected in 9 out of 10 placebo mice while in

**A**

Top Upstream Regulators	
Upstream Regulators	
Upstream Regulator	p-value of overlap
NKX2-5	9.26E-05
FUT7	3.85E-04
YY1AP1	5.76E-04
IL10RA	7.43E-04
CXCL12	1.32E-03

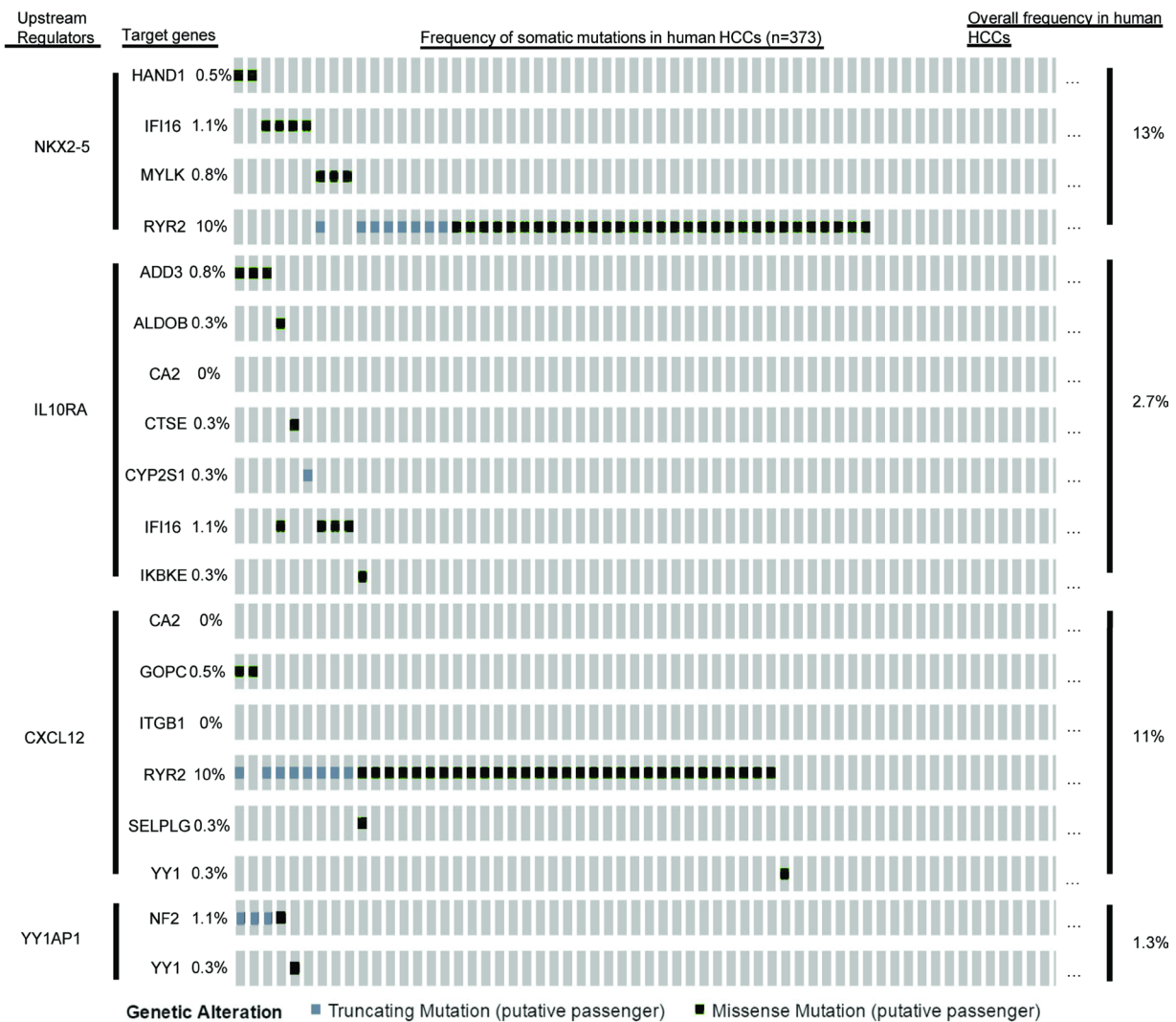
  

Causal Networks	
Name	p-value of overlap
resatorvid	2.51E-06
SIGIRR	2.98E-05
TLR2/TLR4	3.18E-05
CD14/TLR4/LY96	3.50E-05
HSP90B1	5.96E-05

**B**

Upstream Regulators	Target genes in dataset	Frequency in <i>HepPten</i> <sup>-/-</sup> mice
NKX2-5	HAND1	20%
	IFI16	
	MYLK	
	RYR2	
IL10RA	ADD3	40%
	ALDOB	
	CA2	
	CTSE	
	CYP2S1	
	IFI16	
	IKBKE	
CXCL12 (SDF1)	CA2	40%
	GOPC	
	ITGB1	
	RYR2	
	SELPLG	
YY1AP1 (HCCA2)	YY1	20%
	NF2	

**C**



**Figure 1: WES and IPA analysis reveals relevant biological targets of HCC in *HepPten*<sup>-/-</sup> mice.** (A) IPA results of the 162 genes identified mutated in HCC tumors in *HepPten*<sup>-/-</sup> mice. Core analysis on IPA identified top upstream regulators and causal networks for the dataset. (B) Percentage of *HepPten*<sup>-/-</sup> mice that carried a mutation in at least one of the target genes for each identified upstream regulator. (C) Percentage of HCC patients in TCGA that carried a mutation in at least one of the target genes for each identified upstream regulator.

the resatorvid-treated group, only 1 mouse had a detectable small tumor by MRI ( $p < 0.001$ ) (Figure 2A–2B). The average tumor burden in placebo mice was significantly greater than in resatorvid-treated mice at day 14 with  $11.1 \pm 4.8 \text{ mm}^3$  ( $8.4\text{--}44.8 \text{ mm}^3$ ) vs.  $0.0 \pm 0.0 \text{ mm}^3$ , respectively ( $p = 0.022$ ); and at day 28 with  $36.4 \pm 12.0 \text{ mm}^3$  ( $7.5\text{--}114.6 \text{ mm}^3$ ) vs.  $1.0 \pm 1.0 \text{ mm}^3$ , respectively ( $p < 0.001$ ) (Figure 2C).

### Effects of resatorvid treatment on liver steatosis and fibrosis in HepPten<sup>-</sup> mice

Since HepPten<sup>-</sup> mice develop NASH prior to HCC, we also evaluated the effect of resatorvid treatment on this underlying liver pathology. To that end, a liver pathologist analyzed the histology of the liver of the treated mice, blinded to the treatment group. Representative H&E and Masson Trichrome's staining images are shown in Supplementary Figure 1. Compared to resatorvid-treated mice, placebo-treated mice had significantly more macrovesicular steatosis and more steatosis overall, which was often panlobular (i.e., extending from portal tracts to central veins); the resatorvid-treated mice only had mild perivenular (zone 3) microvesicular steatosis. Treatment with resatorvid resulted in a significant decrease in macrovesicular steatosis from a score of  $1.9 \pm 0.4$  to a score of  $0.9 \pm 0.3$  ( $p = 0.031$ ) (Figure 3A). No effect on microvesicular steatosis scores was observed. In addition, the placebo-treated group had more prominent bile ductular reactions and increased periportal, subsinusoidal, and perivenular fibrosis. The bile duct lesions often contained scattered inflammatory cells with surrounding fibrosis. Both subsinusoidal fibrosis and periportal fibrosis were significantly reduced upon resatorvid treatment from a score of  $2.4 \pm 0.2$  to  $1.1 \pm 0.2$  ( $p < 0.001$ ) and from a score of  $1.3 \pm 0.2$  to  $0.6 \pm 0.2$  ( $p = 0.015$ ), respectively (Figure 3B). Bile-ductular reaction was also strongly reduced upon resatorvid treatment ( $p = 0.014$ ) (Figure 3C). No significant effect was observed on hepatocyte ballooning degeneration and inflammation.

### Demographic and clinical characteristics of HCC patients with high tumoral TLR4 mRNA expression

To characterize HCC patients with elevated TLR4 mRNA gene expression in tumors, we retrieved using cBioPortal, clinical, demographic, and mRNA expression data from 363 HCC patients analyzed in The Cancer Genome Atlas (TCGA) (Supplementary Table 2). HCC patients were separated into quartiles, dependent upon respective TLR4 mRNA expression. Groups were dichotomized into “low” versus “high” expression. We defined high TLR4 mRNA expression as quartile Q4 ( $n = 91$ ) and low TLR4 expression as quartiles Q1–Q3

( $n = 272$ ). The demographic and clinical characteristics of HCC patients with elevated TLR4 mRNA expression in tumors are presented in Table 1. After adjustment to age and sex, high TLR4 mRNA expression was strongly associated with NAFLD (AOR = 2.73, 95% CI = 1.09–6.85,  $p = 0.032$ ). High TLR4 mRNA expression was also associated with obesity (adjusted Odds Ratio (AOR) = 2.03, 95% CI = 1.13–3.63,  $p = 0.017$ ). The high TLR4 expression group was less likely to be HBV positive (AOR = 0.47, 95% CI = 0.26–0.88,  $p = 0.017$ ) or to have alpha-feto protein (AFP) blood levels above 20 ng/ml (AOR = 0.56, 95% CI = 0.31–1.01,  $p = 0.055$ ). Finally, we did not find any association with gender, age, HCV, alcohol consumption, presence of cirrhosis or family history of cancer.

### Correlation analysis of TLR4, IL-6 and IL-10 mRNA expression and factors associated with high IL-6 or IL-10 mRNA expression in HCC tumors

To identify companion biomarkers of TLR4 activation in HCC, we performed correlation analyses of tumoral mRNA expression between TLR4 and known TLR4-associated cytokines, IL-6 and IL-10, using the same HCC gene expression dataset from TCGA. TLR4 mRNA expression strongly correlated with IL-6 mRNA expression ( $r = 0.458$ ,  $p < 0.0001$ ) and IL-10 mRNA expression ( $r = 0.452$ ,  $p < 0.0001$ ) (Figure 4). The correlation was even stronger in obese HCC patients ( $n = 66$ ) with  $r = 0.544$ ,  $p < 0.0001$  for IL-6 and  $r = 0.576$ ,  $p < 0.0001$  for IL-10 (Figure 4). HCC patients were again separated into quartiles, by IL-6 or by IL-10 mRNA expression. The demographic and clinical characteristics of HCC patients with elevated IL-6 mRNA expression in tumors are presented in Supplementary Table 3 and summarized in Table 2A. After adjustment for age and sex, high IL-6 mRNA expression was also associated with obesity (AOR = 3.11, 95% CI = 1.74–5.56,  $p = 0.0001$ ) and NAFLD (AOR = 2.59, 95% CI = 1.03–6.52,  $p = 0.042$ ) and inversely associated with HBV (AOR = 0.34, 95% CI = 0.17–0.65,  $p = 0.0013$ ). In addition and in contrast to TLR4, a strong association was found with HCV (AOR = 2.98, 95% CI = 1.61–5.50,  $p = 0.0005$ ). The frequency of HCV was 12.4% in HCC patients with low IL-6 mRNA gene expression but reached 27.9% in the high IL-6 expression group. As for TLR4, we did not find any association with gender, age, alcohol etiology, cirrhosis or family history of cancer. The only significant association found with high IL-10 mRNA expression in HCC tumors was obesity (AOR = 2.34, 95% CI = 1.30–4.23,  $p = 0.004$ ) (Supplementary Table 4 and Table 2B). The frequency of obese individuals in low and high IL-10 mRNA gene expression was 16.5% and 30.9% respectively.



Ob mice, development of steatohepatitis was shown to be dependent on TLR4 [29]. In mice with hepatocyte-deletion of *Pten*, TLR4 but not TLR2 deficiency suppressed tumor growth as well as hepatic inflammation, in good agreement with the results of our study. The authors suggested that TLR4 on macrophages contributes to the development of steatohepatitis-related HCC in this model [30]. Cooperation between TLR4 signaling and STAT3 in promoting tumor-initiating stem-like cells in mouse liver was recently reported [31]. Interestingly, we showed that a small molecule inhibitor of STAT3 blocked HCC tumor growth, reduced tumor development, and improved NASH in *HepPten*- mice, and that these effects were associated with an inhibition of TLR signaling pathways [32]. Future studies should be pursued to identify the TLR4-expressing cells and mechanisms that mediate the chemopreventive effect of resatorvid. Whether the effects of TLR4 on NASH and HCC development in our model are dependent on the gut microbiome should be further investigated. Indeed, emerging data have recently shown a close association between compositional changes in gut microbiota and the development of NAFLD.

Gut microbiota are a source of TLR ligands, and their compositional change can also increase the amount of TLR ligands delivered to the liver. Remarkably, recent studies showed promotion of HCC by the intestinal microbiota and TLR4 [33] and that gut-derived LPS promotes T-cell-mediated hepatitis in mice through TLR4 [34].

To determine who would benefit from TLR4 inhibition treatment for HCC prevention, we characterized using TCGA HCC public datasets, HCC patients with elevated TLR4 mRNA expression as well as HCC patients with elevated mRNA expression of two known cytokines produced by TLR4 activation, IL-6 and IL-10. Among all HCCs, patients with NAFLD and obese patients had the higher tumoral expression of TLR4, IL-6 and IL-10. In addition, TLR4 and IL-6 or IL-10 mRNA expression in tumors were found to strongly correlate in obese HCC patients. Future studies should evaluate the effects of resatorvid in high fat diet induced steatosis and consequent HCC development in mouse models.

Besides TLR4, a number of upstream regulators, potential drivers of HCC in NASH were also identified. NKX2-5 is a transcription factor known to regulate

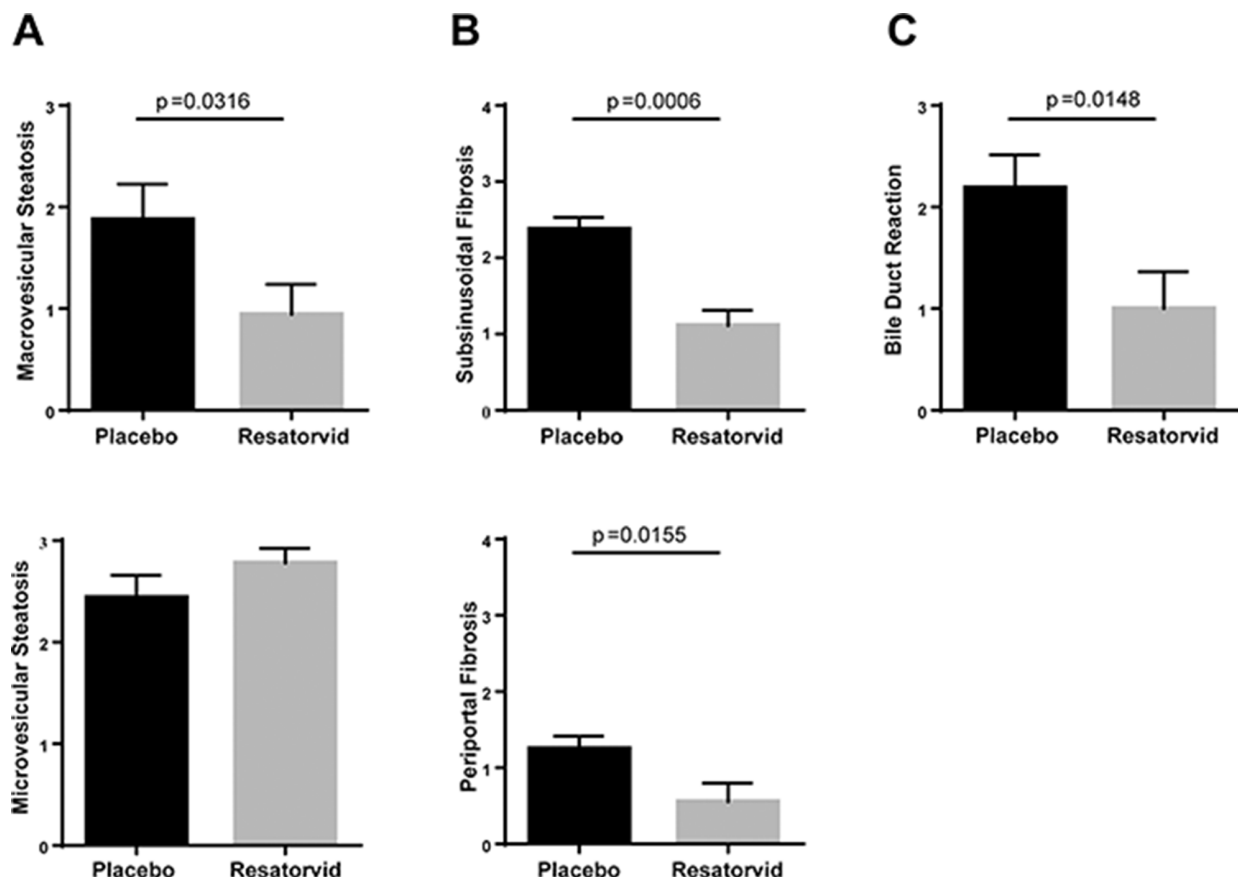


**Figure 3: Effects of resatorvid on steatosis and liver fibrosis in *HepPten* mice.** Livers of placebo and resatorvid-treated mice were analyzed for histopathological features associated with NASH. (A) Macrovesicular steatosis was graded on a 0 to 3 scale (0 for <5%, 1 for 5–33%, 2 for 34–66%, and 3 for >66%). (B) Subsinusoidal and periportal fibrosis were examined and scored using a scoring system of 0 to 4. (C) Bile-duct reaction was assessed based on the number of lesions observed [0 for absent, 1 for 1–4 lesions (focal), 2 for 5–10 lesions (frequent), and 3 for >10 lesions (diffuse)].

**Table 1: Demographic and clinical variables in 363 HCC patients by tumoral TLR4 mRNA expression**

	Low TLR4 (Q1-Q3)	High TLR4 (Q4)	<i>P</i>	Adjusted OR	<i>P</i>
<b>TLR4 mRNA Expression</b> ( <i>n</i> = 363)	152.9 (4.1)–150.1	552.0 (29.6)–452.6			
<b>Male</b> ( <i>n</i> = 363)	181 (66.5%)	63 (69.2%)	0.6366	1.13 (0.68–1.89)	0.6418
<b>Race, Ethnicity</b> ( <i>n</i> = 344)			0.4965		0.503
Asian	122 (47.5%)	34 (39.1%)		REF	
White, Non-Hispanic	111 (43.2%)	44 (50.6%)		1.66 (0.94–2.91)	0.0784
White, Hispanic	10 (3.9%)	5 (5.7%)		1.89 (0.60–5.95)	0.2785
Other	14 (5.4%)	4 (4.6%)		1.04 (0.32–3.39)	0.9459
<b>Age (y)</b> ( <i>n</i> = 363)	59.59 (0.80)–61.0	59.43 (1.38)–61.0	0.9185	1.0 (0.98–1.02)	0.9527
<b>Family History of Cancer</b> ( <i>n</i> = 312)			0.539	1.21 (0.71–2.07)	0.477
	77 (33.9%)	32 (37.6%)			
<b>BMI</b> ( <i>n</i> = 329)	25.4 (0.4)–24.3	26.7 (0.8)–24.7	0.1037	1.04 (0.99–1.08)	0.0922
<b>NAFLD</b> ( <i>n</i> = 344)	11 (4.2%)	9 (10.7%)	0.0329	2.73 (1.09–6.85)	0.0327
<b>Obese (BMI ≥ 30)</b> ( <i>n</i> = 329)	41 (16.9%)	25 (28.7%)	0.0198	2.03 (1.13–3.63)	0.0173
<b>HBV</b> ( <i>n</i> = 344)	86 (33.1%)	17 (20.2%)	0.0272	0.47 (0.26–0.88)	0.0173
<b>HCV</b> ( <i>n</i> = 344)	43 (16.5%)	13 (15.5%)	0.8187	0.90 (0.46–1.78)	0.7591
<b>Alcohol Etiology</b> ( <i>n</i> = 344)	87 (33.5%)	28 (33.3%)	0.9827	0.94 (0.54–1.63)	0.8112
<b>Cirrhosis</b> ( <i>n</i> = 282)	67 (32.4%)	28 (37.3%)	0.436	1.24 (0.71–2.17)	0.4437
<b>Fibrosis</b> ( <i>n</i> = 248)	124 (66.3%)	37 (60.7%)	0.4222	0.78 (0.42–1.45)	0.4238
<b>Fibrosis Ishak Score</b> ( <i>n</i> = 161)			0.0545		0.0503
1, 2	30 (24.2%)	5 (13.5%)		REF	
3, 4	27 (21.8%)	4 (10.8%)		0.93 (0.23–3.88)	0.9246
5, 6	67 (54.0%)	28 (75.7%)		2.78 (0.96–8.05)	0.0596
<b>AFP (ng/mL)</b> ( <i>n</i> = 273)	18202 (9948)–23	877.0 (644.4)–10	0.1911	1.00 (1.00–1.00)	0.2053
<b>AFP ≥ 20 ng/mL</b> ( <i>n</i> = 273)	107 (51.0%)	23 (36.5%)	0.0456	0.56 (0.31–1.01)	0.0555

Data are presented as mean (SEM)-median or as frequency (%). BMI, body mass index; NAFLD, non-alcoholic fatty liver disease; HBV, hepatitis B virus; HCV, hepatitis C virus.

*β*-catenin transcription and with a potential role in HCC development [35]. YY1AP1 was recently identified as an oncogenic driver in EpCam (+) AFP(+) HCC by altering the chromatin landscape and activating stem-like features [36]. IL-10 and associated immune pathway promote a favorable environment for hepatocarcinogenesis thus accelerating HCC progression in NASH [37, 38]. CXCL12 activates CXC chemokine receptor 4 (CXCR4) resulting in

liver fibrosis, tumor growth, and HCC metastasis [39–41]. All these genes should be further investigated.

In conclusion, this study highlighted the specific molecular events and signaling pathways in the pathogenesis of NAFLD-associated HCC and identified the important role of TLR4 in promoting HCC development in the context of NASH. This study demonstrated the promise of using a TLR4 inhibitor such

as resatorvid for HCC chemoprevention and suggested that patients with obesity, diabetes and/or NAFLD should be the target population for this chemoprevention approach. IL-6 or IL-10 could be promising markers to further stratify patients to treat.

## MATERIALS AND METHODS

### Mice: tissue collection, treatment and MR Imaging

C57BL/6 mice with hepatocyte-specific *Pten* deletion (*HepPten*) were crossed with an Albumin (*Alb*)-*Cre*-

transgenic mice. For this model, control animals are *Pten*<sup>loxP/loxP</sup>; *Alb-Cre*<sup>-</sup> while the experimental mice are *Pten*<sup>loxP/loxP</sup>; *Alb-Cre*<sup>+</sup> (*HepPten*). All animal procedures were carried out in accordance with the policies and regulations set forth by the Institutional Animal Care and Use Committee (IACUC) at MD Anderson Cancer Center. At necropsy, tumors and liver tissues were harvested and cut into several sections. These sections were either snap-frozen in liquid nitrogen, fixed in 10% neutral formalin, or embedded in OCT in cryomolds for further analysis. Blood samples were also harvested at necropsy and processed for serum and plasma collection for further analysis. For treatment, resatorvid, also called TAK-242 (Calbiochem, MA, United States), was

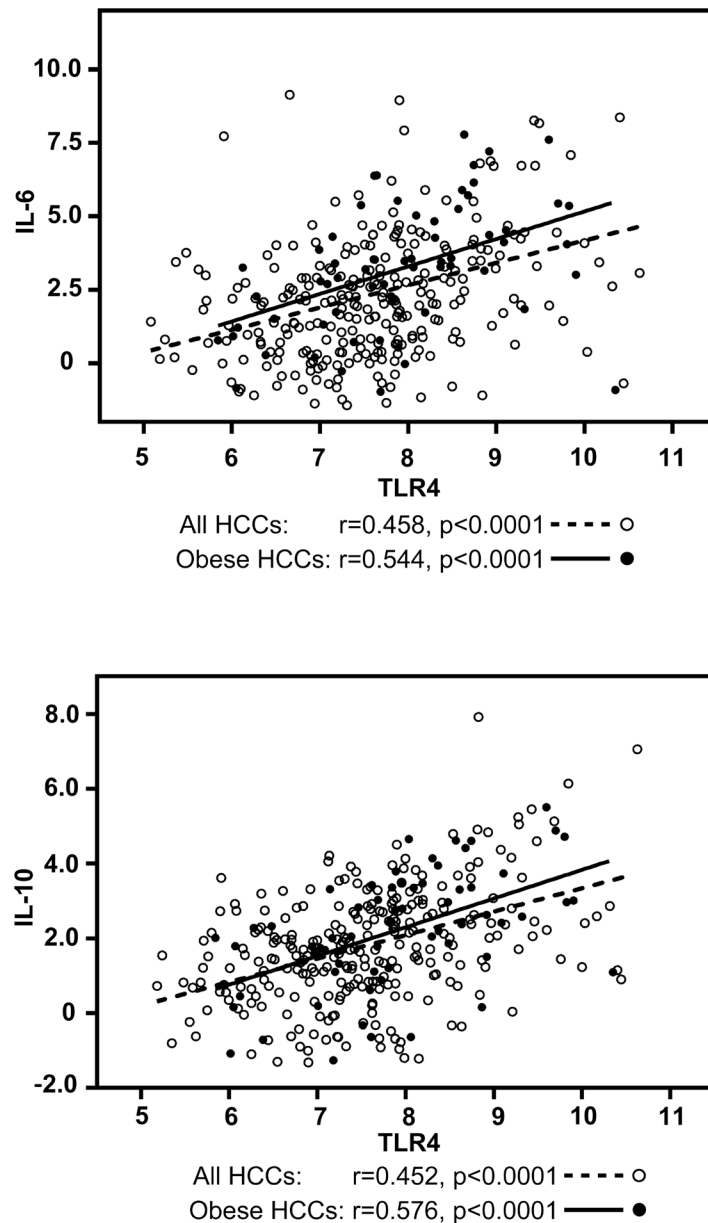


**Figure 4: Correlation analysis between TLR4 and IL-6 / IL-10 mRNA expression in HCC tumors in all HCC patients and in obese HCC patients.** Correlation was evaluated using Spearman rank-order correlation coefficient. Graphs are represented using Log2 values in all HCCs (open dots and dotted lines) and in obese HCCs (dark dots and solid lines).

**Table 2: Demographic and clinical variables in 363 HCC patients by (A) tumoral IL-6 and (B) tumoral IL-10 mRNA expression**

<b>A</b>					
	<b>Low IL-6 (Q1–Q3)</b>	<b>High IL-6 (Q4)</b>	<b>P</b>	<b>Adjusted OR</b>	<b>P</b>
<b>IL6 mRNA Expression (n = 363)</b>	3.19 (0.18)–2.22	63.00 (10.24)–22.01			
<b>BMI (n = 329)</b>	25.1 (0.4)–24.0	27.7 (0.8)–26.3	0.0019	1.07 (1.03–1.11)	0.0018
<b>NAFLD (n = 344)</b>	11 (4.3%)	9 (10.5%)	0.0392	2.59 (1.03–6.52)	0.0427
<b>Obese (BMI ≥ 30) (n = 329)</b>	37 (15.0%)	29 (35.4%)	0.0001	3.11 (1.74–5.56)	0.0001
<b>HBV (n = 344)</b>	90 (34.9%)	13 (15.1%)	0.0008	0.34 (0.17–0.65)	0.0013
<b>HCV (n = 344)</b>	32 (12.4%)	24 (27.9%)	0.0010	2.98 (1.61–5.50)	0.0005
<b>Alcohol Etiology (n = 344)</b>	86 (33.3%)	29 (33.7%)	0.9474	1.14 (0.66–1.99)	0.6418
<b>B</b>					
	<b>Low IL10 (Q1–Q3)</b>	<b>High IL10 (Q4)</b>	<b>P</b>	<b>Adjusted OR</b>	<b>P</b>
<b>IL-10 mRNA Expression (n = 363)</b>	2.47 (0.11)–2.32	18.55 (2.99)–11.05			
<b>BMI (n = 329)</b>	25.3 (0.4)–24.2	27.1 (0.9)–25.0	0.0242	1.05 (1.01–1.10)	0.0153
<b>NAFLD (n = 344)</b>	14 (5.4%)	6 (7.0%)	0.5956	1.33 (0.49–3.59)	0.5726
<b>Obese (BMI ≥ 30) (n = 329)</b>	41 (16.5%)	25 (30.9%)	0.0059	2.34 (1.30–4.23)	0.0046
<b>HBV (n = 344)</b>	83 (32.2%)	20 (23.3%)	0.1198	0.59 (0.33–1.06)	0.0783
<b>HCV (n = 344)</b>	41 (15.95)	15 (17.4%)	0.7360	1.14 (0.59–2.19)	0.7044
<b>Alcohol Etiology (n = 344)</b>	80 (31.0%)	35 (40.7%)	0.1002	1.69 (0.98–2.92)	0.0593

Data are presented as mean (SEM)-median or as frequency (%). BMI, body mass index; NAFLD, non-alcoholic fatty liver disease; HBV, hepatitis B virus; HCV, hepatitis C virus.

dissolved with DMSO to create a 10 mg/ml stock solution and was further diluted with Dulbecco's Phosphate-Buffered Saline for *in vivo* treatment. A total of nineteen 8 month-old *HepPten* male mice were divided into two groups: 1) placebo ( $n = 10$ ) and 2) mice receiving intraperitoneal (IP) injection of resatorvid at a dosage of 10 mg/kg, daily for 28 days ( $n = 9$ ). The Biospec USR47/40 (Bruker Biospin MRI) imaging system was used to image the mice at days 0, 14 and 28. Liver tumors were detected using a standard rapid acquisition with relaxation enhancement (RARE) sequence in the coronal and axial planes with a 250  $\mu$ m slice thickness and with the number of slices sufficient to cover the entire liver. Tumor slice areas were selected, measured with the ROI manager feature of ImageJ and finally used to calculate tumor volume.

### Histopathological evaluation

Formalin-fixed tissue sections were sectioned and subsequently stained with hematoxylin and eosin (H&E) or Masson's Trichome stains. Histopathological features of the

sectioned and stained liver tissues were blindly evaluated by a liver pathologist. The following histopathology parameters were scored: fibrosis (0–4), macrovesicular steatosis (0–3), microvesicular steatosis (0–3), lobular inflammation (0–3), hepatocellular ballooning degeneration (0–2), and bile ductular reaction (0–3).

### Whole-exome sequencing (WES)

DNA was extracted from 20 tumors, distant non tumoral liver and tails collected from 9–12 months male *HepPten* mice ( $n = 10$ ) using QIAmp® DNA Mini Kit. Indexed libraries were prepared from Biorupter Ultrasonicator (Diagenode)-sheared gDNA using the KAPA Hyper Library Preparation Kit (Kapa Biosystems). Library quality was assessed using The NGS Fragment Analyzer Reagent (Advanced Analytical Technologies). The libraries were then prepared for capture with 7 cycles of Ligation Mediated PCR (LM-PCR) amplification. Following Ligation Mediated PCR, amplified libraries were assessed for (i) quality using The NGS Fragment Analyzer Reagent (Advanced

Analytical Technologies) and (ii) quantity using the Qubit dsDNA HS Assay Kit (ThermoFisher), then multiplexed four libraries per pool. Exome capture was performed using the NimbleGen SeqCap EZ Developer Kit. The enriched libraries were PCR amplified 6 cycles post capture and assessed for the quality using The NGS Fragment Analyzer Reagent (Advanced Analytical Technologies). Enrichment of PCR products was assessed by quantitative PCR and quantified using the Qubit dsDNA HS Assay Kit. Sequencing was performed on the HiSeq4000 Sequencer (Illumina Inc) with four samples per lane using the 76nt paired-end configuration. For Single nucleotide variants (SNVs) and small insertions and deletions (indels) identification, Raw BCL files off the sequencer were processed using Illumina's Consensus Assessment of sequence And Variation (CASAVA) tool ([https://support.illumina.com/sequencing/sequencing\\_software/bcl2fastq-conversion-software.html](https://support.illumina.com/sequencing/sequencing_software/bcl2fastq-conversion-software.html)) for demultiplexing/conversion to FASTQ format. The FASTQ files were aligned to the reference genome (mouse mm10) using BWA [42] with 3 mis-matches with 2 in the first 40 seed regions for the 76 bases of the reads. The aligned BAM files were subjected to mark duplication, re-alignment, and re-calibration using Picard and GATK [43] before any downstream analyses. Somatic mutation calls were determined using MuTect [44] followed by functional annotation using ANNOVAR (<http://annovar.openbioinformatics.org/en/latest/>). Nonsynonymous SNVs with mutated allele frequency more than 5% and covered by at least 20 reads in tumor and 10 reads in the matching normal, were used for further analysis. Nonsynonymous somatic indels were filtered and selected for further analysis by mutated allele frequency of 5% or more and covered by at least 20 reads in the tumor and 10 reads in the matching normal. SNVs and somatic indels were further filtered for exonic or splicing function. Qiagen's Ingenuity Pathway Analysis software was used for upstream and causal network analysis. The list of genes carrying at least one somatic mutation in tumors of adult male Hep*Pten*<sup>-</sup> was uploaded and subjected to a core analysis, from which relevant upstream regulators and causal networks were identified.

## Data sources and human subject parameters

The Cancer Genome Atlas (TCGA) HCC data from the cBioPortal online platform (<http://www.cbioportal.org/>) is the source of human subjects parameters. For TCGA HCC, clinical and demographic information as well as mRNA expression for TLR4, IL-6 and IL-10 from 363 HCCs with available mRNA expression profiling data and after exclusion of fibrolamellar carcinomas, were downloaded from cBioPortal (Supplementary Table 2).

## Statistical analysis

Unpaired Mann-Whitney tests were utilized to assess statistical difference between mice groups. Correlation between TLR4, IL6, and IL10 mRNA

expression was evaluated using Spearman rank-order correlation coefficient. In TCGA, we divided the patients into quartiles based on TLR4, IL-6 or IL-10 mRNA expression. For all TCGA analyses, the highest quartiles of expression were compared to the lower three quartiles combined. For crude analysis, we used univariable logistic regression to calculate *p*-values. We then repeated the analyses adjusting for age and gender. All analysis were conducted in SPSS Version 24.0 for Windows. Statistical tests were considered significant at *p* < 0.05.

## Abbreviations

AFP: alpha-feto protein; Alb: albumin; AOR: Adjusted Odds Ratio; APL: Acute Promyelocytic Leukemia; CI: Confidence Interval; CXCL12: C-X-C Motif Chemokine Ligand 12; CXCR4: C-X-C Motif Chemokine Receptor 4; FKBP7: FK506 binding protein 7; FUT7: Fucosyltransferase 7; HBV: Hepatitis B Virus; HCC: Hepatocellular Carcinoma; HCV: Hepatitis C Virus; Hep*Pten*<sup>-</sup>: hepatocyte-specific *Pten* Deletion; IL10: Interleukin 10; IL10RA: Interleukin 10 Receptor Subunit Alpha; IL6: Interleukin 6; IPA: Ingenuity Pathway Analysis; NAFLD: Non-Alcoholic Fatty Liver Disease; NASH: Non-Alcoholic Steatohepatitis; NKX2-5 NK2 homeobox 5; OR: Odds Ratio; SIGIRR: Single immunoglobulin interleukin-1 receptor related molecule; SNP: Single Nucleotide Polymorphism; SNV: Single Nucleotide Variant; TCGA: The Cancer Genome Atlas; TLR4: Toll-like Receptor 4; WES: Whole-Exome Sequencing; YY1API: YY1 Associated Protein 1.

## Author contributions

Conception and design: L.Beretta. Development of methodology: J. Nguyen, J. Jiao, C.Zhao. Acquisition of data: J. Nguyen, J. Jiao. Analysis and interpretation of data: J. Nguyen, X.Song, J.Zhang, K.Smoot, J. Jiao, H.L.Stevenson, G. Watt. Writing, review, and/or revision of the manuscript: L.Beretta, J. Nguyen, K.Smoot, H.L.Stevenson, J. Jiao. Administrative, technical, or material support: H.L.Stevenson, J.B McCormick, S.P. Fisher-Hoch, A. Futreal, and L.Beretta. Study supervision: L.Beretta.

## ACKNOWLEDGMENTS

We would like to thank Dr. Erika J Thompson and Dr. Hongli Tang from the Sequencing and Microarray Facility and Dr. Xizeng Mao from the Department of Genomic Medicine for their help in sequencing and data analysis.

## CONFLICTS OF INTEREST

No potential conflicts of interest were disclosed by authors.

## FUNDING

The study was supported by the NIH/NCI under award number P30CA016672 and use of the Sequencing and Microarray Facility, by UTHealth Innovation for Cancer Prevention Research Training Program Post-doctoral Fellowship (Cancer Prevention and Research Institute of Texas grant # RP160015, to J.J.), by CPRIT-CURE Summer Undergraduate Program at MD Anderson (to K.S.), by a cancer prevention fellowship supported by the National Cancer Institute (grant R25E CA056452, to G.W.), by the Trans-Texas HCC Study and a Start-Up fund from The University of Texas MD Anderson Cancer Center (to L.B).

## REFERENCES

1. Ferlay J, Soerjomataram I, Dikshit R, Eser S, Mathers C, Rebelo M, Parkin DM, Forman D, Bray F. Cancer incidence and mortality worldwide: sources, methods and major patterns in GLOBOCAN 2012. *Int J Cancer*. 2015; 136:E359–86. <https://doi.org/10.1002/ijc.29210>.
2. Wallace MC, Preen D, Jeffrey GP, Adams LA. The evolving epidemiology of hepatocellular carcinoma: a global perspective. *Expert Rev Gastroenterol Hepatol*. 2015; 9:765–79. <https://doi.org/10.1586/17474124.2015.1028363>.
3. Ryerson AB, Ehemann CR, Altekruse SF, Ward JW, Jemal A, Sherman RL, Henley SJ, Holtzman D, Lake A, Noone AM, Anderson RN, Ma J, Ly KN, et al. Annual Report to the Nation on the Status of Cancer, 1975–2012, featuring the increasing incidence of liver cancer. *Cancer*. 2016; 122:1312–37. <https://doi.org/10.1002/cncr.29936>.
4. Pan JJ, Fallon MB. Gender and racial differences in nonalcoholic fatty liver disease. *World J Hepatol*. 2014; 6:274–83. <https://doi.org/10.4254/wjh.v6.i5.274>.
5. Bruix J, Sherman M, American Association for the Study of Liver D. Management of hepatocellular carcinoma: an update. *Hepatology*. 2011; 53:1020–2. <https://doi.org/10.1002/hep.24199>.
6. Kim H, Park YN. Hepatocellular carcinomas expressing ‘stemness’-related markers: clinicopathological characteristics. *Dig Dis*. 2014; 32:778–85. <https://doi.org/10.1159/000368021>.
7. Horie Y, Suzuki A, Kataoka E, Sasaki T, Hamada K, Sasaki J, Mizuno K, Hasegawa G, Kishimoto H, Iizuka M, Naito M, Enomoto K, Watanabe S, et al. Hepatocyte-specific Pten deficiency results in steatohepatitis and hepatocellular carcinomas. *J Clin Invest*. 2004; 113:1774–83. <https://doi.org/10.1172/JCI20513>.
8. Stiles B, Wang Y, Stahl A, Bassilian S, Lee WP, Kim YJ, Sherwin R, Devaskar S, Lesche R, Magnuson MA, Wu H. Liver-specific deletion of negative regulator Pten results in fatty liver and insulin hypersensitivity [corrected]. *Proc Natl Acad Sci U S A*. 2004; 101:2082–7. <https://doi.org/10.1073/pnas.0308617100>.
9. Teufel A, Itzel T, Erhart W, Brosch M, Wang XY, Kim YO, von Schonfels W, Herrmann A, Bruckner S, Stickel F, Dufour JF, Chavakis T, Hellerbrand C, et al. Comparison of Gene Expression Patterns Between Mouse Models of Nonalcoholic Fatty Liver Disease and Liver Tissues From Patients. *Gastroenterology*. 2016; 151:513–25 e0. <https://doi.org/10.1053/j.gastro.2016.05.051>.
10. Wu J. Utilization of animal models to investigate nonalcoholic steatohepatitis-associated hepatocellular carcinoma. *Oncotarget*. 2016; 7:42762–76. <https://doi.org/10.18632/oncotarget.8641>.
11. Lau JK, Zhang X, Yu J. Animal models of non-alcoholic fatty liver disease: current perspectives and recent advances. *J Pathol*. 2017; 241:36–44. <https://doi.org/10.1002/path.4829>.
12. Kawamoto T, Ii M, Kitazaki T, Iizawa Y, Kimura H. TAK-242 selectively suppresses Toll-like receptor 4-signaling mediated by the intracellular domain. *Eur J Pharmacol*. 2008; 584:40–8. <https://doi.org/10.1016/j.ejphar.2008.01.026>.
13. Wald D, Qin J, Zhao Z, Qian Y, Naramura M, Tian L, Towne J, Sims JE, Stark GR, Li X. SIGIRR, a negative regulator of Toll-like receptor-interleukin 1 receptor signaling. *Nat Immunol*. 2003; 4:920–7. <https://doi.org/10.1038/ni968>.
14. Yamamoto M, Sato S, Hemmi H, Hoshino K, Kaisho T, Sanjo H, Takeuchi O, Sugiyama M, Okabe M, Takeda K, Akira S. Role of adaptor TRIF in the MyD88-independent toll-like receptor signaling pathway. *Science*. 2003; 301:640–3. <https://doi.org/10.1126/science.1087262>.
15. Vives-Pi M, Somoza N, Fernandez-Alvarez J, Vargas F, Caro P, Alba A, Gomis R, Labeta MO, Pujol-Borrell R. Evidence of expression of endotoxin receptors CD14, toll-like receptors TLR4 and TLR2 and associated molecule MD-2 and of sensitivity to endotoxin (LPS) in islet beta cells. *Clin Exp Immunol*. 2003; 133:208–18.
16. Ii M, Matsunaga N, Hazeki K, Nakamura K, Takashima K, Seya T, Hazeki O, Kitazaki T, Iizawa Y. A novel cyclohexene derivative, ethyl (6R)-6-[N-(2-Chloro-4-fluorophenyl)sulfamoyl]cyclohex-1-ene-1-carboxylate (TAK-242), selectively inhibits toll-like receptor 4-mediated cytokine production through suppression of intracellular signaling. *Mol Pharmacol*. 2006; 69:1288–95. <https://doi.org/10.1124/mol.105.019695>.
17. Leon CG, Tory R, Jia J, Sivak O, Wasan KM. Discovery and development of toll-like receptor 4 (TLR4) antagonists: a new paradigm for treating sepsis and other diseases. *Pharm Res*. 2008; 25:1751–61. <https://doi.org/10.1007/s11095-008-9571-x>.
18. Matsunaga N, Tsuchimori N, Matsumoto T, Ii M. TAK-242 (resatorvid), a small-molecule inhibitor of Toll-like receptor (TLR) 4 signaling, binds selectively to TLR4 and interferes with interactions between TLR4 and its adaptor molecules. *Mol Pharmacol*. 2011; 79:34–41. <https://doi.org/10.1124/mol.110.068064>.
19. Rice TW, Wheeler AP, Bernard GR, Vincent JL, Angus DC, Aikawa N, Demeyer I, Sainati S, Amlot N, Cao C, Ii M,

- Matsuda H, Mouri K, et al. A randomized, double-blind, placebo-controlled trial of TAK-242 for the treatment of severe sepsis. *Crit Care Med.* 2010; 38:1685–94. <https://doi.org/10.1097/CCM.0b013e3181e7c5c9>.
20. Guo J, Friedman SL. Toll-like receptor 4 signaling in liver injury and hepatic fibrogenesis. *Fibrogenesis Tissue Repair.* 2010; 3: 21. <https://doi.org/10.1186/1755-1536-3-21>.
  21. Pradere JP, Troeger JS, Dapito DH, Mencin AA, Schwabe RF. Toll-like receptor 4 and hepatic fibrogenesis. *Semin Liver Dis.* 2010; 30:232–44.
  22. Roh YS, Seki E. Toll-like receptors in alcoholic liver disease, non-alcoholic steatohepatitis and carcinogenesis. *J Gastroenterol Hepatol.* 2013; 28 Suppl 1:38–42. <https://doi.org/10.1111/jgh.12019>.
  23. Yang J, Li M, Zheng QC. Emerging role of Toll-like receptor 4 in hepatocellular carcinoma. *J Hepatocell Carcinoma.* 2015; 2:11–7. <https://doi.org/10.2147/JHC.S44515>.
  24. Kiziltas S. Toll-like receptors in pathophysiology of liver diseases. *World J Hepatol.* 2016; 8:1354–69. <https://doi.org/10.4254/wjh.v8.i32.1354>.
  25. Jagavelu K, Routray C, Shergill U, O'Hara SP, Faubion W, Shah VH. Endothelial cell toll-like receptor 4 regulates fibrosis-associated angiogenesis in the liver. *Hepatology.* 2010; 52:590–601. <https://doi.org/10.1002/hep.23739>.
  26. Guo J, Loke J, Zheng F, Hong F, Yea S, Fukata M, Tarocchi M, Abar OT, Huang H, Sninsky JJ, Friedman SL. Functional linkage of cirrhosis-predictive single nucleotide polymorphisms of Toll-like receptor 4 to hepatic stellate cell responses. *Hepatology.* 2009; 49:960–8. <https://doi.org/10.1002/hep.22697>.
  27. Minmin S, Xiaoqian X, Hao C, Baiyong S, Xiaying D, Junjie X, Xi Z, Jianquan Z, Songyao J. Single nucleotide polymorphisms of Toll-like receptor 4 decrease the risk of development of hepatocellular carcinoma. *PLoS One.* 2011; 6:e19466. <https://doi.org/10.1371/journal.pone.0019466>.
  28. Kapil S, Duseja A, Sharma BK, Singla B, Chakraborti A, Das A, Ray P, Dhiman RK, Chawla Y. Genetic polymorphism in CD14 gene, a co-receptor of TLR4 associated with non-alcoholic fatty liver disease. *World J Gastroenterol.* 2016; 22:9346–55. <https://doi.org/10.3748/wjg.v22.i42.9346>.
  29. Sutter AG, Palanisamy AP, Lench JH, Jessmore AP, Chavin KD. Development of steatohepatitis in Ob/Ob mice is dependent on Toll-like receptor 4. *Ann Hepatol.* 2015; 14:735–43.
  30. Miura K, Ishioka M, Minami S, Horie Y, Ohshima S, Goto T, Ohnishi H. Toll-like Receptor 4 on Macrophage Promotes the Development of Steatohepatitis-related Hepatocellular Carcinoma in Mice. *J Biol Chem.* 2016; 291:11504–17. <https://doi.org/10.1074/jbc.M115.709048>.
  31. Uthaya Kumar DB, Chen CL, Liu JC, Feldman DE, Sher LS, French S, DiNorcia J, French SW, Naini BV, Junrungsee S, Agopian VG, Zarrinpar A, Machida K. TLR4 Signaling via NANOG Cooperates With STAT3 to Activate Twist1 and Promote Formation of Tumor-Initiating Stem-Like Cells in Livers of Mice. *Gastroenterology.* 2016; 150:707–19. <https://doi.org/10.1053/j.gastro.2015.11.002>.
  32. Jung KH, Yoo W, Stevenson HL, Deshpande D, Shen H, Gagea M, Yoo SY, Wang J, Eckols TK, Bharadwaj U, Twardy DJ, Beretta L. Multifunctional Effects of a Small-Molecule STAT3 Inhibitor on NASH and Hepatocellular Carcinoma in Mice. *Clin Cancer Res.* 2017; 23:5537–46. <https://doi.org/10.1158/1078-0432.CCR-16-2253>.
  33. Dapito DH, Mencin A, Gwak GY, Pradere JP, Jang MK, Mederacke I, Caviglia JM, Khiabani H, Adeyemi A, Batailler R, Lefkowitz JH, Bower M, Friedman R, et al. Promotion of hepatocellular carcinoma by the intestinal microbiota and TLR4. *Cancer Cell.* 2012; 21:504–16. <https://doi.org/10.1016/j.ccr.2012.02.007>.
  34. Lin Y, Yu LX, Yan HX, Yang W, Tang L, Zhang HL, Liu Q, Zou SS, He YQ, Wang C, Wu MC, Wang HY. Gut-derived lipopolysaccharide promotes T-cell-mediated hepatitis in mice through Toll-like receptor 4. *Cancer Prev Res (Phila).* 2012; 5:1090–102. <https://doi.org/10.1158/1940-6207.CAPR-11-0364>.
  35. Liu Y, Ye X, Zhang JB, Ouyang H, Shen Z, Wu Y, Wang W, Wu J, Tao S, Yang X, Qiao K, Zhang J, Liu J, et al. PROX1 promotes hepatocellular carcinoma proliferation and sorafenib resistance by enhancing beta-catenin expression and nuclear translocation. *Oncogene.* 2015; 34:5524–35. <https://doi.org/10.1038/onc.2015.7>.
  36. Zhao X, Parpart S, Takai A, Roessler S, Budhu A, Yu Z, Blank M, Zhang YE, Jia HL, Ye QH, Qin LX, Tang ZY, Thorgeirsson SS, et al. Integrative genomics identifies YY1API as an oncogenic driver in EpCAM(+) AFP(+) hepatocellular carcinoma. *Oncogene.* 2015; 34:5095–104. <https://doi.org/10.1038/onc.2014.438>.
  37. Ouyang FZ, Wu RQ, Wei Y, Liu RX, Yang D, Xiao X, Zheng L, Li B, Lao XM, Kuang DM. Dendritic cell-elicited B-cell activation fosters immune privilege via IL-10 signals in hepatocellular carcinoma. *Nat Commun.* 2016; 7:13453. <https://doi.org/10.1038/ncomms13453>.
  38. Ambade A, Satishchandran A, Saha B, Gyongyosi B, Lowe P, Kodys K, Catalano D, Szabo G. Hepatocellular carcinoma is accelerated by NASH involving M2 macrophage polarization mediated by hif-1alpha-induced IL-10. *Oncoimmunology.* 2016; 5:e1221557. <https://doi.org/10.1080/2162402X.2016.1221557>.
  39. Liu H, Pan Z, Li A, Fu S, Lei Y, Sun H, Wu M, Zhou W. Roles of chemokine receptor 4 (CXCR4) and chemokine ligand 12 (CXCL12) in metastasis of hepatocellular carcinoma cells. *Cell Mol Immunol.* 2008; 5:373–8. <https://doi.org/10.1038/cmi.2008.46>.
  40. Liu Y, Yang X, Jing Y, Zhang S, Zong C, Jiang J, Sun K, Li R, Gao L, Zhao X, Wu D, Shi Y, Han Z, et al. Contribution and Mobilization of Mesenchymal Stem Cells in a mouse model of carbon tetrachloride-induced liver fibrosis. *Sci Rep.* 2015; 5: 17762. <https://doi.org/10.1038/srep17762>.

41. Shah AD, Bouchard MJ, Shieh AC. Interstitial Fluid Flow Increases Hepatocellular Carcinoma Cell Invasion through CXCR4/CXCL12 and MEK/ERK Signaling. *PLoS One*. 2015; 10:e0142337. <https://doi.org/10.1371/journal.pone.0142337>.
42. Li H, Durbin R. Fast and accurate short read alignment with Burrows-Wheeler transform. *Bioinformatics*. 2009; 25:1754–60. <https://doi.org/10.1093/bioinformatics/btp324>.
43. DePristo MA, Banks E, Poplin R, Garimella KV, Maguire JR, Hartl C, Philippakis AA, del Angel G, Rivas MA, Hanna M, McKenna A, Fennell TJ, Kernysky AM, et al. A framework for variation discovery and genotyping using next-generation DNA sequencing data. *Nat Genet*. 2011; 43:491–8. <https://doi.org/10.1038/ng.806>.
44. Cibulskis K, Lawrence MS, Carter SL, Sivachenko A, Jaffe D, Sougnez C, Gabriel S, Meyerson M, Lander ES, Getz G. Sensitive detection of somatic point mutations in impure and heterogeneous cancer samples. *Nat Biotechnol*. 2013; 31:213–9. <https://doi.org/10.1038/nbt.2514>.